

# Quasi-relativistic behavior of cold atoms in light fields

Gediminas Juzeliūnas,<sup>1</sup> Julius Ruseckas,<sup>1</sup> Markus Lindberg,<sup>2</sup> Luis Santos,<sup>3</sup> and Patrik Öhberg<sup>4</sup>

<sup>1</sup>*Institute of Theoretical Physics and Astronomy of Vilnius University, A. Goštauto 12, Vilnius 01108, Lithuania*

<sup>2</sup>*Department of Physics, Åbo Akademi University, Åbo FIN-20500, Finland*

<sup>3</sup>*Institut für Theoretische Physik, Leibniz Universität, Hannover D30167, Germany*

<sup>4</sup>*SUPA, School of Engineering and Physical Sciences, Heriot-Watt University, Edinburgh EH14 4AS, United Kingdom*

(Dated: October 27, 2018)

We study the influence of three laser beams on the center of mass motion of cold atoms with internal energy levels in a tripod configuration. We show that similar to electrons in graphene the atomic motion can be equivalent to the dynamics of ultra-relativistic two-component Dirac fermions. We propose and analyze an experimental setup for observing such a quasi-relativistic motion of ultracold atoms. We demonstrate that the atoms can experience negative refraction and focussing by Veselago-type lenses. We also show how the chiral nature of the atomic motion manifests itself as an oscillation of the atomic internal state population which depends strongly on the direction of the center of mass motion. For certain directions an atom remains in its initial state, whereas for other directions the populations undergo oscillations between a pair of internal states.

PACS numbers: 03.75.-b, 39.25.+k, 42.50.Gy, 42.25.Bs

## INTRODUCTION

Two-dimensional (2D) quantum systems are a source of many remarkable phenomena. A striking example in this respect is provided by the properties of electrons in graphene [1, 2, 3, 4, 5, 6, 7, 8, 9] — a two dimensional hexagonal crystal of carbon atoms. Near the Fermi level the electrons in graphene behave like massless ultra-relativistic two-component Dirac fermions [10] moving with a velocity  $v_F$  which does not depend on the momentum. This leads to a number of distinct effects in graphene and graphene bilayers, such as a half integer quantum Hall effect [1, 4, 5] and the Klein paradox [3]. Furthermore it has been suggested recently that electrons in graphene should exhibit a negative refraction [8, 9] at a potential barrier, similar to the electromagnetic waves refracting in a counterintuitive way at an interface with a material characterized by a negative dielectric permittivity and a negative magnetic permeability [11, 12].

In this Rapid Communication we show how cold atoms obtain ultra-relativistic properties of Dirac fermions if manipulated by laser beams. We suggest to use three laser beams acting on atoms in a tripod configuration [13, 14]. The light beams induce an effective vector potential (the Mead-Berry connection [15, 16, 17]) which influences the atomic center of mass motion [14]. We demonstrate that by choosing proper light fields the vector potential can be made proportional to an operator of spin 1/2. For small momenta the atomic motion becomes equivalent to the ultra-relativistic motion of two-component Dirac fermions, as is the case for electrons in graphene. We propose and analyze an experimental setup for observing such a quasi-relativistic behavior of the cold atoms. We show that the atoms can experience negative refraction and focussing by Veselago-type lenses [11].

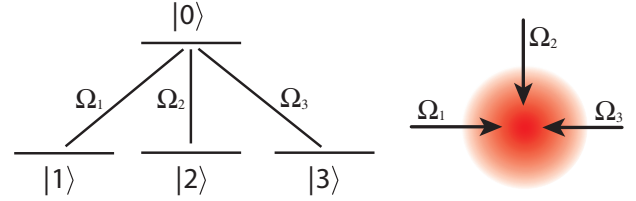


FIG. 1: (Color online) An atom interacting with three laser fields in a tripod configuration.

Interestingly the velocity of the quasi-relativistic atoms is of the order of a centimeter per second. This is ten orders of magnitude smaller than the speed of light in vacuum  $c \approx 3 \times 10^8$  m/s. For comparison, the velocity of the Dirac-type electrons in graphene  $v_F \approx 10^6$  m/s is only three hundred times smaller than  $c$  [4]. Thus the ultra-relativistic behavior of cold atoms manifests itself at extremely small velocities. Note also that our proposal does not need a lattice and thus operates in a continuous regime in contrast to recent papers on the quasi-relativistic dynamics of cold atoms in one-dimensional [18] or 2D hexagonal (graphene-type) [19] lattices.

## FORMULATION

Let us consider the adiabatic motion of atoms in the field of three stationary laser beams. The beams couple four internal atomic levels in a tripod configuration [13, 14], in which the atoms are characterized by three lower levels  $|1\rangle$ ,  $|2\rangle$  and  $|3\rangle$  and an excited level  $|0\rangle$  shown in Fig. 1a [20]. The  $j$ -th laser induces a transition (with a Rabi frequency  $\Omega_j$ ) between the  $j$ -th lowest level and the excited level  $|0\rangle$ . We shall be interested in a scheme where the first two lasers have the same intensities and

counter-propagate in the  $x$ -direction while the third one propagates in the negative  $y$ -direction (see Fig. 1b), i.e.  $\Omega_1 = \Omega \sin \theta e^{-i\kappa x}/\sqrt{2}$ ,  $\Omega_2 = \Omega \sin \theta e^{i\kappa x}/\sqrt{2}$  and  $\Omega_3 = \Omega \cos \theta e^{-i\kappa y}$ , where  $\Omega = \sqrt{|\Omega_1|^2 + |\Omega_2|^2 + |\Omega_3|^2}$  is the total Rabi frequency, and the mixing angle  $\theta$  defines the relative intensity.

The electronic Hamiltonian of the tripod atom reads in the interaction representation [14]

$$\hat{H}_0 = -\hbar(\Omega_1|0\rangle\langle 1| + \Omega_2|0\rangle\langle 2| + \Omega_3|0\rangle\langle 3|) + \text{H.c.} \quad (1)$$

The Hamiltonian  $\hat{H}_0$  has two eigen-states of zero energy containing no contribution from the excited state  $|0\rangle$ :

$$|D_1\rangle = \frac{1}{\sqrt{2}}e^{-i\kappa y} (e^{i\kappa x}|1\rangle - e^{-i\kappa x}|2\rangle) \quad (2)$$

$$|D_2\rangle = \frac{1}{\sqrt{2}}e^{-i\kappa y} \cos \theta (e^{i\kappa x}|1\rangle + e^{-i\kappa x}|2\rangle) - \sin \theta|3\rangle$$

The states  $|D_1\rangle$  and  $|D_2\rangle$  known as the dark states [13, 14] depend on the atomic position through the spatial dependence of the Rabi-frequencies  $\Omega_j$ .

The adiabatic approximation is carried out neglecting transitions from the dark states to the bright state  $|B\rangle \sim \Omega_1^*|1\rangle + \Omega_2^*|2\rangle + \Omega_3^*|3\rangle$ . The latter is coupled to the excited atomic state  $|0\rangle$  with the Rabi frequency  $\Omega$ , so the two states  $|B\rangle$  and  $|0\rangle$  split into a doublet separated from the dark states by the energies  $\pm\Omega$ . The adiabatic approximation is justified if  $\Omega$  is sufficiently large compared to the two-photon detuning due to the laser mismatch and/or Doppler shift. In that case the internal state of an atom evolves within the dark state manifold. The atomic state-vector  $|\Phi\rangle$  can then be expanded in terms of the dark states according to  $|\Phi\rangle = \sum_{j=1}^2 \Psi_j(\mathbf{r})|D_j(\mathbf{r})\rangle$ , where  $\Psi_j(\mathbf{r})$  is the wave-function for the center of mass motion of the atom in the  $j$ -th dark state.

Thus atomic center of mass motion is described by a two-component wave-function  $\Psi = (\Psi_1, \Psi_2)^T$ . The column-matrix  $\Psi$  obeys the Schrödinger equation [14]

$$i\hbar \frac{\partial}{\partial t} \Psi = \left[ \frac{1}{2m}(-i\hbar\nabla - \mathbf{A})^2 + V + \Phi \right] \Psi, \quad (4)$$

where  $m$  is the atomic mass, and  $\mathbf{A}$ ,  $\Phi$  and  $V$  are  $2 \times 2$  matrices. The gauge potentials  $\mathbf{A}$  and  $\Phi$  emerge due to the spatial dependence of the atomic dark states. The reduced  $2 \times 2$  matrix  $\mathbf{A}$  with the elements  $\mathbf{A}_{n,m} = i\hbar \langle D_n(\mathbf{r}) | \nabla D_m(\mathbf{r}) \rangle$  represents the effective vector potential known as the Mead-Berry connection [14, 15, 16, 17]. The  $2 \times 2$  matrix  $\Phi$  acts as an effective scalar potential. The external potential  $V$  confines the motion of the dark-state atoms to a finite region in space. Specifically we have  $V_{n,m} = \langle D_n(\mathbf{r}) | \hat{V} | D_m(\mathbf{r}) \rangle$  with  $\hat{V} = V_1(\mathbf{r})|1\rangle\langle 1| + V_2(\mathbf{r})|2\rangle\langle 2| + V_3(\mathbf{r})|3\rangle\langle 3|$ , where  $V_j(\mathbf{r})$  is the trapping potential for an atom in the internal state  $j = 1, 2, 3$ . Note that the potential  $V_j$  can also accommodate a possible detuning of the  $j$ -th laser from the resonance of the  $j \rightarrow 0$  transition.

## ATOMIC MOTION IN THE FIELD OF THREE PLANE WAVES

The potentials  $\mathbf{A}$ ,  $\Phi$  and  $V$  have been considered in Ref. [14] for arbitrary light fields. In the present configuration of the light fields, the potentials take the form

$$\mathbf{A} = \hbar\kappa \begin{pmatrix} \mathbf{e}_y & -\mathbf{e}_x \cos \theta \\ -\mathbf{e}_x \cos \theta & \mathbf{e}_y \cos^2 \theta \end{pmatrix}, \quad (5)$$

$$\Phi = \begin{pmatrix} \hbar^2 \kappa^2 \sin^2 \theta / 2m & 0 \\ 0 & \hbar^2 \kappa^2 \sin^2(2\theta) / 8m \end{pmatrix}, \quad (6)$$

$$V = \begin{pmatrix} V_1 & 0 \\ 0 & V_1 \cos^2 \theta + V_3 \sin^2 \theta \end{pmatrix}, \quad (7)$$

where the external trapping potential is assumed to be the same for the first two atomic states,  $V_1 = V_2$ .

In what follows we take  $V_3 - V_1 = \hbar^2 \kappa^2 \sin^2(\theta) / 2m$ . This can be achieved by detuning the third laser from the two-photon resonance by the frequency  $\Delta\omega_3 = \hbar\kappa^2 \sin^2 \theta / 2m$ . Thus the overall trapping potential simplifies to  $V + \Phi = V_1 \mathbf{I}$  (up to a constant), where  $\mathbf{I}$  is the unit matrix. In other words, both dark states are affected by the same trapping potential  $V_1 \equiv V_1(\mathbf{r})$ .

Furthermore we take the mixing angle  $\theta = \theta_0$  to be such that  $\sin^2 \theta_0 = 2 \cos \theta_0$ , giving  $\cos \theta_0 = \sqrt{2} - 1$ . In that case the vector potential can be represented in a symmetric way in terms of the Pauli matrices  $\sigma_x$  and  $\sigma_z$

$$\mathbf{A} = \hbar\kappa'(-\mathbf{e}_x \sigma_x + \mathbf{e}_y \sigma_z) + \hbar\kappa_0 \mathbf{e}_y \mathbf{I}, \quad (8)$$

where  $\kappa' = \kappa \cos \theta_0 \approx 0.414\kappa$  and  $\kappa_0 = \kappa(1 - \cos \theta_0)$ . Although the vector potential is constant, it can not be eliminated via a gauge transformation, because the Cartesian components  $A_x$  and  $A_y$  do not commute. Thus the light-induced potential  $\mathbf{A}$  is non-Abelian. Note that non-Abelian gauge potentials can also be induced in optical lattices using other techniques [21].

It is convenient to introduce new dark states:

$$|D'_1\rangle = \frac{1}{\sqrt{2}}(|D_1\rangle + i|D_2\rangle) e^{i\kappa_0 y}, \quad (9)$$

$$|D'_2\rangle = \frac{i}{\sqrt{2}}(|D_1\rangle - i|D_2\rangle) e^{i\kappa_0 y}. \quad (10)$$

The transformed two component wave-function is related to the original one according to  $\Psi' = \exp(-i\kappa_0 y) \exp(-i\frac{\pi}{4}\sigma_x) \Psi$ . The exponential factor  $\exp(-i\kappa_0 y)$  induces a shift in the origin of the momentum  $\mathbf{k} \rightarrow \mathbf{k} - \kappa_0 \mathbf{e}_y$ . With the new set of dark states we get the vector potential  $\mathbf{A}' = -\hbar\kappa' \sigma_\perp$ , where  $\sigma_\perp = \mathbf{e}_x \sigma_x + \mathbf{e}_y \sigma_y$  is the spin 1/2 operator in the  $xy$  plane. The transformed equation of the atomic motion takes the form

$$i\hbar \frac{\partial}{\partial t} \Psi' = \left[ \frac{1}{2m}(-i\hbar\nabla + \hbar\kappa' \sigma_\perp)^2 + V_1 \right] \Psi'. \quad (11)$$

In this way the vector potential governing the atomic motion is proportional to the spin operator  $\sigma_\perp$ .

If the trapping potential  $V_1$  is constant, we can consider plane-wave solutions,

$$\Psi'(\mathbf{r}, t) = \Psi_{\mathbf{k}} e^{i\mathbf{k}\cdot\mathbf{r} - i\omega_{\mathbf{k}}t}, \quad \Psi_{\mathbf{k}} = \begin{pmatrix} \Psi_{1\mathbf{k}} \\ \Psi_{2\mathbf{k}} \end{pmatrix}, \quad (12)$$

where  $\omega_{\mathbf{k}}$  is the eigen-frequency. The  $\mathbf{k}$ -dependent spinor  $\Psi_{\mathbf{k}}$  obeys the stationary Schrödinger equation  $H_{\mathbf{k}}\Psi_{\mathbf{k}} = \hbar\omega_{\mathbf{k}}\Psi_{\mathbf{k}}$ , with the following  $\mathbf{k}$ -dependent Hamiltonian

$$H_{\mathbf{k}} = \frac{\hbar^2}{2m}(\mathbf{k} + \kappa'\sigma_{\perp})^2 + V_1. \quad (13)$$

For small wave-vectors ( $k \ll \kappa'$ ) the atomic Hamiltonian reduces to the Hamiltonian for the 2D relativistic motion of a two-component massless particle of the Dirac type known also as the Weyl equation [22],

$$H_{\mathbf{k}} = \hbar v_0 \mathbf{k} \cdot \sigma_{\perp} + V_1 + m v_0^2, \quad (14)$$

where  $v_0 = \hbar\kappa'/m$  is the velocity of such a quasi-relativistic particle. The velocity  $v_0$  represents the recoil velocity corresponding to the wave-vector  $\kappa'$ , and is typically of the order of a centimeter per second.

The Hamiltonian  $H_{\mathbf{k}}$  commutes with the 2D chirality operator  $\sigma_{\mathbf{k}} = \mathbf{k} \cdot \sigma_{\perp}/k$ . The later has the eigenstates

$$\Psi_{\mathbf{k}}^{\pm} = \frac{1}{\sqrt{2}} \begin{pmatrix} 1 \\ \pm \frac{k_x + ik_y}{k} \end{pmatrix}, \quad (15)$$

for which  $\sigma_{\mathbf{k}}\Psi_{\mathbf{k}}^{\pm} = \pm\Psi_{\mathbf{k}}^{\pm}$ . Here the chirality is associated with the subspace of the dark states defined by the basis in Eqs. (9)–(10) rather than with the spin states in the usual sense. The corresponding dynamics can therefore also be illustrated by for instance a Poincaré sphere.

The eigenstates (15) are also eigenstates of the Hamiltonian  $H_{\mathbf{k}}$  with eigen-frequencies  $\omega_{\mathbf{k}} \equiv \omega_{\mathbf{k}}^{\pm}$ . In what follows the atomic motion is assumed to be confined in the  $xy$  plane. The dispersion then reads

$$\hbar\omega_{\mathbf{k}}^{\pm} = \hbar v_0(k^2/2\kappa' \pm k) + V_1 + m v_0^2, \quad (16)$$

see Fig. 2 in which  $V_1 = -m v_0^2/2$ . The atomic motion in different dispersion branches is characterized by opposite chirality if the direction  $\mathbf{k}/k$  is fixed. For small wave-vectors ( $k \ll \kappa'$ ) the dispersion simplifies to  $\hbar\omega_{\mathbf{k}}^{\pm} = \pm\hbar v_0 k + V_1 + m v_0^2$ , where the upper (lower) sign corresponds to a linear cone with a positive (negative) group velocity,  $v_g^{\pm} = \pm v_0$ . Exactly the same dispersion is featured for electrons near the Fermi level in graphene [1, 2, 3, 4, 5].

## PROPOSED EXPERIMENT

To observe the quasi-relativistic behavior of cold atoms, we propose the following experimental situation. We suppose initially an atom (or a dilute atomic cloud)

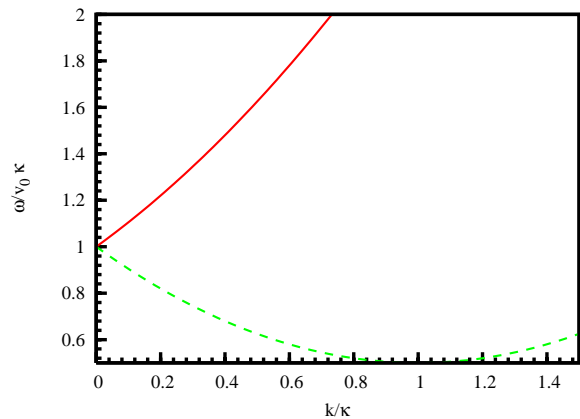


FIG. 2: (Color online) Upper (red solid) and lower (green dashed) dispersion branches for a tripod atom in light fields

is in the internal state  $|3\rangle$  with a translational motion described by a wave-packet with a central wave-vector  $\mathbf{k}_{\text{in}}$  and a wave-vector spread  $\Delta k \ll k_{\text{in}}$ , i.e.  $|\Psi_{\text{in}}\rangle = \psi(\mathbf{r})e^{i\mathbf{k}_{\text{in}}\cdot\mathbf{r}}|3\rangle$ , where the envelope function  $\psi(\mathbf{r})$  varies slowly within the wavelength  $\lambda_{\text{in}} = 2\pi/k_{\text{in}}$ . The cold atoms can be set in motion using various techniques, e.g. by means of the two-photon scattering which induces a recoil momentum  $\hbar\mathbf{k}_{\text{in}} = \hbar\mathbf{k}_{2\text{phot}}$  to the atoms, where  $\mathbf{k}_{2\text{phot}}$  is a wave-vector of the two-photon mismatch [23].

Initially all three lasers are off. Subsequently the lasers are switched on in a counterintuitive manner, switching the lasers 1 and 2 on first followed by the laser 3. At the beginning of this stage the internal state  $|3\rangle$  coincides with the dark state  $|D_2\rangle$ , so the original and transformed multi-component wave-functions are given by:

$$\Psi = \begin{pmatrix} 0 \\ 1 \end{pmatrix} \psi(\mathbf{r})e^{i\mathbf{k}_{\text{in}}\cdot\mathbf{r}}, \quad \Psi' = \frac{1}{\sqrt{2}} \begin{pmatrix} -i \\ 1 \end{pmatrix} \psi(\mathbf{r})e^{i\mathbf{k}\cdot\mathbf{r}}, \quad (17)$$

where the transformed wave-function  $\Psi'$  is obtained expressing the original dark state  $|D_2\rangle$  through the new ones  $|D'_{1,2}\rangle$ , with  $\mathbf{k} = \mathbf{k}_{\text{in}} - \kappa_0\mathbf{e}_y$  being a new central wave-vector. If the laser 3 is switched on sufficiently slowly, the atom remains in the dark state  $|D_2\rangle$  during the whole switch-on stage. Yet the duration of the switching on should be short enough to prevent the dynamics of the atomic center of mass at this stage. To have ultra-relativistic behaving atoms, the wave-number  $k$  should be small  $k \ll \kappa$ , so that  $\mathbf{k}$  is a small contribution to  $\mathbf{k}_{\text{in}} = \kappa_0\mathbf{e}_y + \mathbf{k}$ . In addition, the wave-number spread  $\Delta k \ll k$ , i.e. the width of the atomic wave-packet is much larger than the central wave-length. The subsequent centre of mass motion of atoms in the laser fields is sensitive to the direction of the wave-vector  $\mathbf{k}$ .

(i) If  $\mathbf{k} = \pm k\mathbf{e}_y$ , the wave-function (17) reads:

$$\Psi' = -i\Psi_{\mathbf{k}}^{\pm}\psi(\mathbf{r})e^{\pm ik_y}, \quad \Psi_{\mathbf{k}}^{\pm} = \frac{1}{\sqrt{2}} \begin{pmatrix} 1 \\ i \end{pmatrix}. \quad (18)$$

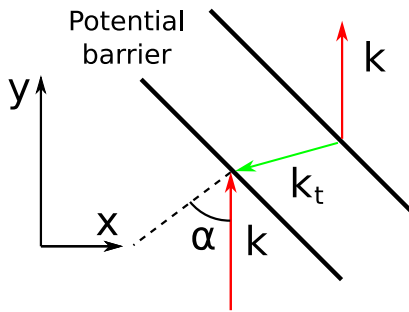


FIG. 3: (Color online) Negative refraction of cold atoms at a potential barrier. The incoming and outgoing atoms are in the upper (red) dispersion branch, whereas the atoms inside the barrier are in the lower (green) one.

The upper (lower) sign in  $\mathbf{k} = \pm k\mathbf{e}_y$  corresponds to a situation where the atom is characterized by a positive (negative) chirality, hence being in the upper (lower) dispersion branch. In both cases the atomic wave-packet propagates along the  $y$  axis with the velocity  $\mathbf{v}_0 = \mathbf{e}_y \hbar \kappa' / m$ .

(ii) If the wave-vector is along the  $x$  axis ( $\mathbf{k} = k\mathbf{e}_x$ ), the multi-component wave-function (17) takes the form

$$\Psi' = (c_+ \Psi_{\mathbf{k}}^+ + c_- \Psi_{\mathbf{k}}^-) \psi(\mathbf{r}) e^{i\mathbf{k} \cdot \mathbf{r}}, \quad \Psi_{\mathbf{k}}^{\pm} = \frac{1}{\sqrt{2}} \begin{pmatrix} 1 \\ \pm 1 \end{pmatrix}, \quad (19)$$

where  $c_{\pm} = (-i \pm 1)/2$ . In that case the initial wave-packet splits into two with equal weights ( $|c_{\pm}| = 1/2$ ) and the same wave-vector  $\mathbf{k}$ . The wave-packets are characterized by different chiralities and thus move in opposite directions with the velocities  $\mathbf{v}_0 = \pm \mathbf{e}_x \hbar \kappa' / m$ .

Suppose the time is sufficiently small ( $v_0 t < d$ ), so the wave-packets of the width  $d$  are not yet spatially separated. The internal atomic state will then undergo temporal oscillations between the dark states  $|D_2\rangle$  and  $|D_1\rangle$  with a frequency equal to  $\omega_{\mathbf{k}}^+ - \omega_{\mathbf{k}}^- = 2v_0 k$ . Such an internal dynamics can be detected by switching the laser 3 off at a certain time. This transforms the dark state  $|D_2\rangle$  to the physical state  $|3\rangle$ . Subsequently one can measure population of the state  $|3\rangle$  for various delay times and various wave-vectors  $\mathbf{k}$ . The chiral nature of the atomic motion will manifest itself in the oscillations of the population of the atomic state  $|3\rangle$  if  $\mathbf{k}$  is along the  $x$  axis, and the absence of such oscillations if  $\mathbf{k}$  is along the  $y$  axis.

Furthermore as a consequence of the constructed Hamiltonian (14), the quasi-relativistic atoms can show negative refraction at a potential barrier and thus exhibit focussing by Veselago-type lenses [11, 12]. Consider incident atoms that are in the upper dispersion branch and propagate along the  $y$  axis with a wave-vector  $\mathbf{k} = k\mathbf{e}_y$ . Let us place a potential barrier of a height  $2\hbar v_0 k$  at an angle of incidence  $\alpha$  (see Fig. 3). Inside the barrier the atoms are transferred to the lower dispersion branch with  $\mathbf{k}_t = -k[\cos(2\alpha)\mathbf{e}_y + \sin(2\alpha)\mathbf{e}_x]$ . This would lead to the

negative refraction of cold atoms at the barrier as shown in Fig. 3. Thus the potential barrier can act as a flat lens which refocuses the atomic wave-packet.

In summary we have shown how the atomic motion can be equivalent to the dynamics of ultra-relativistic (massless) two-component Dirac fermions. As a result the ultracold atoms can experience negative refraction and focusing by Veselago-type lenses. In addition, we have investigated another manifestation of the chiral nature of the atomic motion through dynamics of the population of the internal atomic states.

This work was supported by DFG (SFB407, SPP1116), the Royal Society of Edinburgh and the UK Engineering and Physical Sciences Research Council. We thank A. Matulis for stimulating discussions on graphene, and D. Boiron, J. Arlt and E. Tiemann for information about experimental realizations.

- 
- [1] K. S. Novoselov *et al*, *Nature* **438**, 197 (2005).
  - [2] E. McCann and V. I. Fal'ko, *Phys. Rev. Lett.* **96**, 086805 (2006).
  - [3] M. I. Katsnelson, K. S. Novoselov, and A. K. Geim, *Nature Physics* **2**, 620 (2006).
  - [4] A. K. Geim and K. S. Novoselov, *Nature Materials* **6**, 183 (2007).
  - [5] K. S. Novoselov *et al*, *Science* **315**, 1379 (2007).
  - [6] A. Matulis and F. M. Peeters, *Phys. Rev. B* **75**, 125429 (2007).
  - [7] R. Jackiw and S.-Y. Pi, *Phys. Rev. Lett.* **98**, 266402 (2007).
  - [8] J. B. Pendry, *Science* **315**, 1226 (2007).
  - [9] V. V. Cheianov, V. Fal'ko and B. L. Altshuler, *Science* **315**, 1252 (2007).
  - [10] V. V. Beresteckii, E. M. Lifshitz and L. P. Pitaevskii, *Quantum Electrodynamics* (Oxford, Butterworth Heinemann, 1982).
  - [11] V. G. Veselago, *Sov. Phys. Usp.* **10**, 509 (1968).
  - [12] J. B. Pendry, *Phys. Rev. Lett.* **85**, 3966 (2000).
  - [13] R. G. Unanyan, M. Fleischhauer, B. E. Shore, and K. Bergmann, *Opt. Commun.* **155**, 144 (1998).
  - [14] J. Ruseckas, G. Juzeliūnas, P. Öhberg, and M. Fleischhauer, *Phys. Rev. Lett.* **95**, 010404 (2005).
  - [15] M. V. Berry, *Proc. R. Soc. A* **392**, 45 (1984).
  - [16] F. Wilczek and A. Zee, *Phys. Rev. Lett.* **52**, 2111 (1984).
  - [17] C. A. Mead, *Rev. Mod. Phys.* **64**, 51 (1992).
  - [18] J. Ruostekoski, G. V. Dunne, and J. Javanainen, *Phys. Rev. Lett.* **88**, 180401 (2002).
  - [19] S. L. Zhu, B. G. Wang, L. M. Duan, *Phys. Rev. Lett.* **98**, 260402 (2007).
  - [20] For example, the transition  $2^3S_1 \leftrightarrow 2^3P_0$  in  $^4\text{He}^*$ , or transition  $5S_{1/2} (F=1) \leftrightarrow 5P_{3/2} (F=0)$  in  $^{87}\text{Rb}$ .
  - [21] K. Osterloh, M. Baig, L. Santos, P. Zoller, and M. Lewenstein, *Phys. Rev. Lett.* **95**, 010403 (2005).
  - [22] M. Maggiore, *A Modern Introduction to Quantum Field Theory*, p. 55 (Oxford University Press, Oxford, 2005).
  - [23] See e.g. L. Deng *et al.*, *Nature* **398**, 218 (1999).